Approximate Optimal Distributed Control of Nonlinear Interconnected Systems Using Event-Triggered Nonzero-Sum Games

Vignesh Narayanan, *Member, IEEE*, Avimanyu Sahoo, *Member, IEEE*, Sarangapani Jagannathan, *Fellow, IEEE*, and Koshy George, *Senior Member, IEEE*

***Abstract*— In this paper, approximate optimal distributed control schemes for a class of nonlinear interconnected systems with strong interconnections are presented using continuous and event-sampled feedback information. The optimal control design is formulated as an *N*-player nonzero-sum game where the control policies of the subsystems act as players. An approximate Nash equilibrium solution to the game, which is the solution to the coupled Hamilton–Jacobi equation, is obtained using the approximate dynamic programming-based approach. A critic neural network (NN) at each subsystem is utilized to approximate the Nash solution and novel event-sampling conditions, that are decentralized, are designed to asynchronously orchestrate the sampling and transmission of state vector at each subsystem. To ensure the local ultimate boundedness of the closed-loop system state and NN parameter estimation errors, a hybrid-learning scheme is introduced and the stability is guaranteed using Lyapunov-based stability analysis. Finally, implementation of the proposed event-based distributed control scheme for linear interconnected systems is discussed. For completeness, Zeno-free behavior of the event-sampled system is shown analytically and a numerical example is included to support the analytical results.**

***Index Terms*— Adaptive dynamic programming (ADP), event-triggered control, interconnected systems, nonzero sum (NZS) game, optimal control.**

I. Introduction

IN THIS digital era, large-scale interconnected systems are prevalent due to the ease of feedback communication among the subsystems over a network. Commonly encountered interconnected systems include electric power grid [1], network controlled systems [2], wireless sensor networks, and so on. The interconnection or the coupling among subsystems affects the subsystem and the overall system behavior. Therefore, the interconnections play a critical role in the design of controllers to meet stability and performance requirements. The controller design techniques for such interconnected systems have been widely studied [1], [3]–[11] and can be classified as decentralized [3]–[6] and distributed [1], [7]–[10] control schemes.

In the decentralized framework [5], [6], the controller at each subsystem uses the local feedback information under the assumption that the interconnection terms are weak in nature. In general, robust/adaptive control techniques [12], [13] or neural network (NN)-based approximate control techniques [5], [6] are used to design the control policies and compensate for the subsystem interconnections. Although decentralized control methods [5], [6] assure stability of the interconnected system, the transient performance of the large-scale system deteriorates and becomes unacceptable when the interconnections among subsystems become strong [8]. In contrast, performance of the subsystems can be improved by employing the distributed control approach [1], [8]–[10] wherein the local subsystem controllers use the state vector of both the local and neighboring subsystems, periodically [9] or intermittently [1], [8], [10].

Performance of an isolated system, i.e., without interconnection/coupling with other systems, can be optimized by solving the associated Riccati equation (RE) for linear systems or the Hamilton–Jacobi–Bellman (HJB) equation for nonlinear systems. Obtaining a closed-form analytical solution for the HJB partial differential equation is not possible [14], and hence, approximate dynamic programming (ADP) [15]–[17]/reinforcement learning (RL) [18], [19] based approximate solutions are sought for optimal control of nonlinear systems.

The ADP/RL-based methods are also extended to decentralized control of interconnected systems (see [3], [4], [11], and the references therein). Mehraeen and Jagannathan [3] proposed a decentralized near-optimal control scheme using neurodynamic programming, in discrete-time, for an interconnected system with unknown nonlinear subsystem dynamics and weak interconnection strength. Liu *et al.* [4] presented an ADP-based decentralized optimal control design using policy iteration wherein the local cost functions for the

Manuscript received December 21, 2017; revised May 31, 2018 and August 15, 2018; accepted September 2, 2018. Date of publication October 8, 2018; date of current version April 16, 2019. This work was supported in part by the Intelligent Systems Center, Missouri University of Science and Technology, Rolla, MO, USA, in part by NSF ECCS under Grant 1406533, in part by CMMI under Grant 1547042, and in part by the start-up fund Oklahoma State University, Stillwater, OK 74078 USA. *(Corresponding author: Avimanyu Sahoo.)*

V. Narayanan is with the Department of Electrical and Systems Engineering, Washington University in St. Louis, St. Louis, MO 63130 USA (e-mail: vnxv4@mst.edu).

A. Sahoo is with the Division of Engineering Technology, Oklahoma State University, Stillwater, OK 74078 USA (e-mail: avimanyu.sahoo@okstate.edu).

S. Jagannathan is with the Department of Electrical and Computer Engineering, Missouri University of Science and Technology, Rolla, MO 65409 USA (e-mail: sarangap@mst.edu).

K. George is with the Department of Electronics and Communication Engineering, PES University, Bengaluru 560085, India (e-mail: kgeorge@pes.edu).

Color versions of one or more of the figures in this paper are available online at http://ieeexplore.ieee.org.

Digital Object Identifier 10.1109/TNNLS.2018.2869896

isolated subsystems are considered to design local optimal controllers. The resulting control policies are suboptimal due to the compensation for the interconnections. On the other hand, optimal distributed control of interconnected systems [3], [4], [7], [11] is a challenging problem [20] due to the difficulty involved in determining a tradeoff between the performance of the overall and the individual subsystems, as well as the communication requirement between subsystems.

Event-based sampling, transmission, and control execution [10], [21] schemes are found to be more promising in reducing the communication/computational resource utilization. Furthermore, event-based ADP schemes for isolated systems [1], [22]–[24] are also successful in reducing the computational complexity of the control schemes. In our previous effort [7], [25], [26], event-based approximate optimal control schemes for interconnected systems are proposed. Lyapunov-based decentralized event-triggering conditions are derived such that the resulting aperiodic implementation of the distributed control policies ensures stability of the overall system. Despite ensuring stability and minimizing a desired performance index of the overall system [7], [25], [26], the centralized cost function used to design the controllers at each subsystem does not have the flexibility to optimize the performance of individual subsystems, independently. As a consequence, improving the performance of one subsystem can result in degradation of the performance of the other subsystems. In a nutshell, the optimal control of interconnected systems formulated either based on a global [3], [7] or local objective functions [4] leads to the optimization of either the local or overall system performance and not both.

In practice, subsystems of a large-scale interconnected system may have varied objectives and the control scheme should meet the individual subsystem performance requirements while achieving a global objective. In this context, the theory of multiplayer nonzero-sum (NZS) differential games [27], where each player has a different performance index, is apt to optimize both the individual subsystem and the overall system performance. The set of optimal control polices, referred to as Nash equilibrium policies [28], does not allow any individual player to gain advantage by independently modifying its policy [28]. In other words, for an interconnected system, performance of one subsystem cannot be independently optimized at the expense of the performance of the other subsystems. However, the multiplayer NZS game-based optimal control schemes [29], [30] are studied for multi-input and multioutput systems without any communication involved. Extension of the existing multiplayer control schemes for distributed control of interconnected systems requires a formidable amount of communication resources [10].

Motivated by the above challenges, in this paper, the distributed control of interconnected systems is formulated as a multiplayer NZS game. For the ease of exposition, the distributed optimal control design with continuous transmission of state information among the subsystems is presented first and then extended to the case of event-based sampling, transmission, and control execution. A multiplayer cost function, utilizing the control inputs as players, is defined at each subsystem. The ADP-based approximate solution for the game is designed with both continuous and event-based feedback. NNs [31] are introduced at each subsystem to learn the solution to the coupled Hamilton–Jacobi (HJ) equation online.

A novel continuous update rule is designed to learn the Nash equilibrium solution and to guarantee the learning accuracy in the event-based sampling framework. A hybrid learning [25] approach is adopted to tune the NN weights. To ensure asynchronous triggering, novel decentralized event-triggering conditions using exponential functions are introduced. Finally, the results are extended for linear interconnected systems.

The main contributions of this paper include: 1) distributed optimal control synthesis of interconnected systems offering a tractable tradeoff between the performance of a subsystem and its overall system; 2) approximate solution of the coupled HJ equation as a function of strong interconnections with different control coefficient functions; 3) development of the hybrid NN weight adaptation rule to minimize the Bellman residual error; 4) design of novel, decentralized, and asynchronous event-based sampling conditions to orchestrate the events; and 5) demonstration of the ultimate boundedness (UB) of the closed-loop system parameters with the Zeno-free behavior.

In the remainder of this paper, the problem statement and the proposed solution are presented in Section II. In Section III, a learning scheme to obtain the Nash solution, for the continuous time system, is presented followed by the event-based implementation in Section IV. The special case of linear interconnected system is also discussed in Section IV. Simulation results are included in Section V followed by conclusions in Section VI.

II. Problem Statement and Proposed Solution

A. Problem Statement

Consider an interconnected system consisting of N subsystems, each of which is represented as

$$\dot{x}_i(t) = \bar{f}_i(x_i) + \bar{g}_i(x_i)u_i(x) + \sum_{\substack{j=1\\ j\neq i}}^{N} \Delta_{ij}(x_i, x_j) \tag{1}$$

for $i = 1, 2, \ldots, N$, where $x_i(t) \in \Re^{n_i}$ with $x_i(0) = x_0$, and $u_i(t) \in \Re^{m_i}$ are the state and control policies of the ith subsystem, respectively. The functions $\bar{f}_i : \Re^{n_i} \to \Re^{n_i}$ and $\bar{g}_i : \Re^{n_i} \to \Re^{n_i \times m_i}$ are the internal dynamics and control coefficient of the i^{th} subsystem, respectively, with $\bar{f}_i(0) = 0$. The function $\Delta_{ij} : \Re^{n_i} \times \Re^{n_j} \to \Re^{n_i}$ represents the interconnection between the i^{th} and the j^{th} subsystem.

To stabilize the i^{th} subsystem, the control policy u_i is desired to be a function of $x_i(t)$ and $x_j(t)$ for all j satisfying $\Delta_{ij} \neq 0$ (i.e., distributed control policy) [8]. Therefore, the control objective is to design N distributed optimal control policies $(u_1^*, u_2^*, \ldots, u_N^*)$ such that the following performance index is optimized:

$$J_i(x) = \int_t^{\infty} \left(Q_i(x) + \sum_{j=1}^{N} u_j^T R_{ij} u_j \right) d\tau \tag{2}$$

where $x = [x_1^T, \ldots, x_N^T]^T$ is the overall system state vector, $Q_i(\cdot) \in \Re$ is a positive-definite function with $Q_i(0) = 0$, $R_{ii} \in \Re^{m_i \times m_i}$ is a positive-definite matrix, and $R_{ij} \in \Re^{m_j \times m_j}$ are symmetric matrices for $i = 1, 2, \ldots, N$.

Remark 1: The performance index in (2) is different from the traditionally considered local cost function [4] taking the form $J_i(x_i) = \int_t^\infty (Q_i(x_i) + u_i^T R_i u_i) d\tau$ and the overall system cost function, i.e., $J(x) = \int_t^\infty (Q(x) + u^T R u) d\tau = \sum_{i=1}^N J_i(x)$ [25] with the assumption that the overall cost is a sum of the local costs. A major limitation of these local and global performance indices is that the influence of the neighboring subsystem's policies is not accounted in the subsystem optimization. As a result, optimizing the performance of one subsystem can result in the degradation of the performance of the other subsystems. However, the performance index in (2) is defined in the subsystem level and accounts for all control policies. Therefore, the resulting Nash solution is the optimal solution for both the subsystem and the overall system.

Moreover, in an event-based control paradigm, each subsystem determines the aperiodic sampling and transmission instants to broadcast its state information. Consider the sequence of time instants $\{t_k^i\}_{k=0}^\infty$ with $t_0^i = 0$ for all $i = 1, 2, \ldots, N$ as the event-sampling instants. Then, the states $x_i(t_k^i)$ and $x_j(t_k^j)$ of the i^{th} and j^{th} subsystems are broadcasted at the time instant t_k^i and t_k^j, respectively. Therefore, the solution to the HJ equation must be approximated with the intermittent and asynchronous state information.

In summary, the problem in hand includes: 1) reformulation of the distributed optimal control problem as an NZS game and derive the coupled HJ equation corresponding to the performance index (2) at each subsystem; 2) obtaining a solution to the resulting coupled HJ equation with intermittent availability of the state information and execute the optimal control policy at the aperiodic sampling instants; and 3) designing the asynchronous event-triggering scheme to reduce computations and transmissions at each subsystem while avoiding the Zeno-behavior. The solution to above problems is presented in the following.

B. Proposed Solution

In this section, first, the subsystem dynamics in (1) are augmented to represent an N-player interconnected system and the corresponding coupled HJ equation for (2) is derived. Then, the solution to the resulting optimal control problem is proposed using the game theory.

The interconnected system, by augmenting the subsystem dynamics, can be represented as an N-player system given by

$$\dot{x} = f(x) + \sum_{j=1}^N g_j(x_j) u_j, \quad x(0) = x_0 \tag{3}$$

where $x(t) = [x_1^T, \ldots, x_N^T]^T \in \Re^n$ with $n = \sum_{i=1}^N n_i$ is the augmented state of the large-scale system. The map $f(x) = [(\bar{f}_1(x_1) + \sum_{j=2}^N \Delta_{1j}(x))^T, \ldots, (\bar{f}_N(x_N) + \sum_{j=1}^{N-1} \Delta_{Nj}(x))^T]^T$ with $f(0) = 0$ and $g_j(x_j) = [0, \ldots, \bar{g}_j^T(x_j), \ldots, 0]^T \in \Re^{n \times m_j}$, $j = 1, \ldots, N$ are the known overall internal dynamics and the control coefficient function, where 0s are matrices with all elements zero.

Assumption 1: The individual subsystems (1) and the augmented system in (3) are stabilizable, and the state vector, x, is available for measurement.

Assumption 2: The functions $\bar{f}_i(x_i)$, $\Delta_{ij}(x_i, x_j)$, and $\bar{g}_i(x_i)$ are locally Lipschitz continuous for all $x \in B_x$, where B_x is a compact set. In addition, the control coefficient matrix $g_i(x_i)$ satisfies $0 < g_{im} < \|g_i(x_i)\| \le g_{iM}$, $i = 1, 2, \ldots, N$ for some constants $g_{im} > 0$ and $g_{iM} > 0$, where $\|\cdot\|$ denotes the Frobenius norm for matrices and the Euclidean norm for vectors.

The optimal value function, V_i^* for $i = 1, \ldots, N$, is given by $V_i^*(x) = \min_{u_i} J_i(x) = \min_{u_i} \int_t^\infty (Q_i(x) + \sum_{j=1}^N u_j^T R_{ij} u_j) d\tau$. By the definition of Nash equilibrium [27], with the optimal N-tuple $\{u_1^*, \ldots, u_N^*\}$, the optimal value at each subsystem satisfies $V_i^* = V_i^*(u_1^*, u_2^*, \ldots, u_N^*) \le V_i^*(u_1^*, \ldots, u_i, \ldots, u_N^*)$, for $i \in \{1, \ldots, N\}$.

Using the infinitesimal version of (2) with the dynamic state constraint (3), the Hamiltonian function H_i is defined as

$$H_i\big(x, u_1, \ldots, u_N, V_{ix}^*\big) = Q_i(x) + \sum_{j=1}^N u_j^T R_{ij} u_j + V_{ix}^{*T}\left[f(x) + \sum_{j=1}^N g_j(x_j) u_j\right] \tag{4}$$

where $V_{ix} = \partial V_i / \partial x$, $i = 1, 2, \ldots, N$. Applying the stationarity condition $\partial H_i / \partial u_i = 0$ reveals the greedy distributed optimal control policy u_i^* given by

$$u_i^* = -(1/2) R_{ii}^{-1} g_i^T V_{ix}^*, \quad \forall i \in \{1, 2, \ldots, N\}. \tag{5}$$

Inserting the optimal control policy (5) into the Hamiltonian function (4) reveals the coupled HJ equations as

$$\begin{aligned} H_i\big(x, u_1^*, \ldots, u_N^*, V_{ix}^*\big) &= Q_i(x) + V_{ix}^{*T}\left[f(x) - \frac{1}{2}\sum_{j=1}^N g_j R_{jj}^{-1} g_j^T V_{jx}^*\right] \\ &\quad + \frac{1}{4}\sum_{j=1}^N V_{jx}^* g_j R_{jj}^{-1} R_{ij} R_{jj}^{-1} g_j^T V_{jx}^{*T} = 0 \\ &\quad \forall i \in \{1, 2, \ldots, N\}. \end{aligned} \tag{6}$$

The optimal control policy for the large-scale system (3) can be obtained using (5) at each subsystem, given the system dynamics and the optimal value function. However, with complete information of the system dynamics in (3), a closed-form solution of the coupled HJ partial differential equation (6), i.e., the optimal value function, is difficult to compute. In general, approximate solution to the HJ equation is sought using the ADP-based approach presented in the following.

III. Approximate Solution to the NZS Game

In this section, continuous availability of the subsystem state information at every subsystem is assumed, which is relaxed in Section IV-A.

A. Value Function Approximation (Critic Design)

The optimal value function, which is the solution to the coupled HJ equation (6), is approximated using a linearly parametrized dynamic NN at each subsystem. The standard assumption on the existence of the solution to the HJ equation is formally stated as follows to proceed.

Assumption 3: The solution to the HJ equation (6), i.e., the optimal value function, $V_i^*(\cdot)$, exists and is unique, real-valued, and continuously differentiable for all $x \in B_x \subseteq \Re^n$.

By the universal approximation property of the NNs [31], there exists an ideal weight matrix $\theta_i^* \in \Re^{l_\theta}$ and a basis function $\phi(x) \in \Re^{l_\theta}$ such that the smooth optimal value function $V_i^*(x)$ can be represented as

$$V_i^*(x) = \theta_i^{*^T}\phi(x) + \varepsilon_i(x), \quad \forall i \in \{1, 2, \ldots, N\} \tag{7}$$

where $\varepsilon_i(x)$ is the approximation error. Note that each subsystem has a value function approximator (critic NN) to approximate the solution of the HJ equation using the input of the overall state $x(t)$. The optimal control policy, using (7), can be expressed as

$$u_i^* = -(1/2)R_{ii}^{-1}g_i^T\left(\nabla_x^T\phi(x)\theta_i^* + \nabla_x\varepsilon_i(x)\right) \tag{8}$$

for $i = 1, 2, \ldots, N$, where $\nabla_x(\cdot) = \partial(\cdot)/\partial x$. The standard assumptions that are used in the analysis are stated next.

Assumption 4 [31]: NN target weight matrix θ_i^*, activation function $\phi(.)$, gradient of activation function $\nabla_x\phi(.)$, reconstruction error $\varepsilon_i(.)$, and the gradient of the reconstruction error $\nabla_x\varepsilon_i(.)$, $\forall i \in \{1, \ldots, N\}$ are bounded satisfying $\|\theta_i^*\| \le \theta_{iM}$, $\phi(.) \le \phi_M$, $\nabla_x\phi(.) \le \nabla\phi_M$, $\|\varepsilon_i(.)\| \le \varepsilon_{iM}$, and $\nabla_x\varepsilon_i(.) \le \nabla\varepsilon_{iM}$, where θ_{iM}, ϕ_M, $\nabla\phi_M$, ε_{iM}, and $\nabla\varepsilon_{iM}$ are positive constants.

Since the target weight of the NN approximation in (7) is unknown, one needs to estimate the NN weights online. The estimate of the optimal value function can be expressed as

$$\hat{V}_i(x) = \hat{\theta}_i^T(t)\phi(x), \quad \forall i \in \{1, \ldots, N\} \tag{9}$$

where $\hat{\theta}_i(t) \in \Re^{l_\theta}$ is the estimate of the target weight θ_i^*. The estimated control policy using (9) is represented as

$$\hat{u}_i = -(1/2)R_{ii}^{-1}g_i^T\hat{V}_{ix} = -(1/2)R_{ii}^{-1}g_i^T\nabla_x^T\phi(x)\hat{\theta}_i. \tag{10}$$

To update the weights of the NN, we will avail the Bellman optimality principle [29]. From (2) and for $T > 0$, we have the recursive Bellman equation

$$V_i^*(x(t)) = \int_t^{t+T}\left(Q_i(x) + \sum_{j=1}^N u_j^T R_{ij}u_j\right)d\tau + V_i^*(x(t+T)). \tag{11}$$

Taking one step backward, we can rewrite (11) using the estimated value as

$$\hat{V}_i(x(t-T)) = \int_{t-T}^t\left(Q_i(x) + \sum_{j=1}^N u_j^T R_{ij}u_j\right)d\tau + \hat{V}_i(x(t)) - E_{ib} \tag{12}$$

where E_{ib} is the temporal difference/Bellman residual error due to the estimated values.

The NN weights can be updated to minimize the function $E_{i_{HJ}} = (1/2)E_{ib}^2$ and learn the optimal value function. For instance, let the NN weight update rule be given by

$$\dot{\hat{\theta}}_i = -\alpha_{i1}(\partial E_{ib}/\partial\hat{\theta}_i)E_{ib} \tag{13}$$

where $\alpha_{i1} = \alpha_i/\rho_i^2$ with $\alpha_i > 0$ is the learning gain and $\rho_i = 1 + (\partial E_{ib}/\partial\hat{\theta}_i)^T(\partial E_{ib}/\partial\hat{\theta}_i)$ is the normalization term.

To facilitate the stability proof, presented in Section III-B, define the NN weight estimation error $\tilde{\theta}_i = \theta_i^* - \hat{\theta}_i$. The weight estimation error dynamics from (13) is given as

$$\dot{\tilde{\theta}}_i = \alpha_{i1}(\partial E_{ib}/\partial\hat{\theta}_i)E_{ib}. \tag{14}$$

B. Stability Analysis

Before claiming uniform ultimate boundedness (UUB) of the closed-loop parameters, the following technical lemmas are required.

Lemma 1: Consider the NN tuning rule (13) and the weight estimation error dynamics (14). With the Bellman equation (12), the weight estimation error dynamics satisfies

$$\dot{L}_i(\tilde{\theta}_i) \le -\frac{\alpha_{i1}}{2}\tilde{\theta}_i^T\Delta\phi(x,T)\Delta\phi^T(x,T)\tilde{\theta}_i + \frac{\alpha_{i1}}{2}\varepsilon_{ib}^T\varepsilon_{ib} \tag{15}$$

for $i \in \{1, \ldots, N\}$, where $L_i(\tilde{\theta}_i) = (1/2)\tilde{\theta}_i^T\tilde{\theta}_i$, $\Delta\phi(x,T) = \phi(x(t)) - \phi(x(t-T))$, and $\varepsilon_{ib} = \varepsilon_i(x(t)) - \varepsilon_i(x(t-T))$.

Proof: Refer to the Appendix.

Remark 2: The approximation error, ε_{ib}, can be reduced by increasing the number of hidden layer neurons [31].

Lemma 2: Given the interconnected system (1) with the optimal control policy u_j^*, $j = 1, 2, \ldots, N$ in (5). Let Assumptions 1–3 hold. Then, for the set of continuously differentiable, radially unbounded Lyapunov candidate functions $L_i(x_i)$ corresponding to each subsystem (1), there exists constants $C_{i2} > 0$ such that the inequality

$$\sum_{i=1}^N L_{ix_i}^T(x_i)\left(\bar{\bar{f}}_i(x) + \bar{g}_i u_i^*\right) \le -\sum_{i=1}^N C_{i2}\|L_{ix_i}(x_i)\|^2 \tag{16}$$

holds, where $\bar{\bar{f}}_i(x) = \bar{f}_i(x_i) + \sum_{j=1, i\neq j}^N \Delta_{ij}(x_i, x_j)$ and $L_{ix_i}(x_i) = \partial L_i(x_i)/\partial x_i$.

Proof: The proof is a direct result of the stabilizing property of the optimal policies $u_i^*(x)$; refer to [15] for details.

Next, for completeness, the definition of the persistence of excitation (PE) condition [31] is presented, which is used for ensuring the stability of the closed-loop system presented in the theorem.

Definition 1: A signal $(\Delta\phi(x,T)/(1 + \Delta\phi^T(x,T)\,\Delta\phi(x,T)))$ is said to be persistently exciting over an interval $[t-T, t]$, if $\forall t \in \Re^+$, there exists a $T > 0, \tau_1 > 0, \tau_2 > 0$ such that $\tau_1 I \leq \int_{t-T}^{t} (\Delta\phi(x,T)\Delta\phi^T(x,T)/((1+\Delta\phi^T(x,T)\Delta\phi(x,T))^2))d\tau \leq \tau_2 I$, where I is the identity matrix of appropriate dimension.

Theorem 1: Consider the interconnected system with the i^{th} subsystem dynamics given by (1) and represented as an N-player large-scale system in (3). Let Assumptions 1-4 hold, and the critic NN weights are initialized in a compact set $\Omega_\theta \subseteq \Re^{l_\theta}$ and updated according to (13). Then, the estimated control input (10) renders the closed-loop system locally uniformly ultimately bounded, provided the design parameters $\beta_i > (\bar{D}_{iM}^2/2C_{i2})$, $\alpha_i > (\nabla\phi_M \beta_i^2/2)$, and the regression vector is persistently exciting, where $\bar{D}_{iM}, \beta_i$ are positive constants.

Proof: Refer to the Appendix.

Corollary 1: Let the hypothesis of Theorem 1 holds. Then, the estimated value function (9) and the control policy (10) converge to an arbitrarily close neighborhood of the optimal value function (7) and control policy (8), respectively.

Proof: Refer to the Appendix.

Next, the Nash solution in the context of the event-based sampling scheme is presented.

IV. Event-Based Approximate Nash Solution

In this section, the assumption of continuous availability of system state vector is relaxed by introducing an asynchronous event-based sampling and transmission scheme among the subsystems. Before presenting the event-sampled formulation, the following property of the communication network is assumed.

Assumption 5: The communication network used for the exchange of feedback information is ideal, i.e., there are no delays and packet losses occurring during transmission.

A. Event-Sampled Optimal Control Policy

Define the local state information received at the i^{th} controller and transmitted to the other subsystems at the occurrence of an event as

$$x_{ie}(t) = x_i(t_k^i), \quad t_k^i \leq t < t_{k+1}^i \quad \forall k. \tag{17}$$

This intermittent transmission of the system state vector introduces an error, referred to as event-sampling error, and is defined as $e_i(t) = x_i(t) - x_{ie}(t)$, $t_k^i \leq t < t_{k+1}^i$, $\forall k \in \{0, \mathbb{N}\}$ and it is reset to zero upon receiving the new state information. The sampling instants t_k^i and t_k^j for $i \neq j$ are asynchronous and are solely governed by the local event-sampling condition at each subsystem defined later in (25).

Remark 3: To implement the distributed controller in the event-based sampling context, the broadcasted state information are stored at each subsystem controller and updated as soon as the new state information is received. However, each subsystem controller is executed only at the local subsystem sampling instants with the latest information available from the local and the neighboring subsystems.

The optimal control policy (5) in the event-sampling context can be rewritten as

$$u_{ie}^* = -\frac{1}{2} R_{ii}^{-1} g_i^T(x_{ie}) V_{ix_e}^*, \quad i = 1, 2, \ldots, N \tag{18}$$

where $x_e = [x_{1e}^T, \ldots, x_{Ne}^T]^T$ is the event-based state vector available at the controller of each subsystem and $V_{ix_e}^* = \partial V_i^*(x)/\partial x\,|_{x=x_e}$. Event-sampled approximation [32] of the optimal value function $V_i^*(x)$ using the NNs is represented as

$$V_i^*(x) = \theta_i^{*^T}\phi(x_e) + \varepsilon_{ie}(x_e, e), \quad i = 1, 2, \ldots, N \tag{19}$$

where $\phi(x_e)$ is the event-sampled activation function and $\varepsilon_{ie}(x_e, e) = \theta_i^{*^T}(\phi(x_e+e) - \phi(x_e)) + \varepsilon_i(x_e+e)$ is the event-sampled approximation error with $e = [e_1^T, \ldots, e_N^T]^T$ being the augmented event-sampling error.

The optimal control policy with event-based state information in a parametric form, for each subsystem, is given as

$$u_{ie}^* = -\frac{1}{2} R_{ii}^{-1} g_{ie}^T \left[\nabla_{x_e}^T \phi(x_e)\theta_i^* + \nabla_{x_e}\varepsilon_{ie}(x_e, e)\right] \tag{20}$$

where $g_{je} = g_j(x_{je})$ and $\nabla_{x_e} = \partial(\cdot)/\partial x\,|_{x=x_e}$.

The estimate of the approximate optimal value function in the event-sampling context can be expressed as

$$\hat{V}_i(x) = \hat{\theta}_i^T(t)\phi(x_e) \tag{21}$$

and the estimated control policy $\hat{u}_{ie}$ is represented as

$$\hat{u}_{ie} = -\frac{1}{2} R_{ii}^{-1} g_{ie}^T \hat{V}_{ix_e} = -\frac{1}{2} R_{ii}^{-1} g_{ie}^T \nabla_{x_e}^T \phi(x_e)\hat{\theta}_i \tag{22}$$

for $i = 1, 2, \ldots, N$.

To derive the NN learning rule, rewrite the Bellman equation (12) in the event-driven framework as

$$\hat{V}_i\left(x\left(t_{k-1}^i\right)\right) = \int_{t_{k-1}^i}^{t_k^i} \left(Q_i(x) + \sum_{j=1}^{N} u_j^T R_{ij} u_j\right) d\tau + \hat{V}_i\left(x\left(t_k^i\right)\right) - E_{ib,e} \tag{23}$$

where $E_{ib,e}$ is the event-driven temporal difference error/Bellman residual error.

Remark 4: Note that the states of the i^{th} subsystem are accessed by the controller located at the i^{th} subsystem at event triggering instants t_k^i only; therefore, it is natural to consider calculating the temporal difference/Bellman residual error at the event-triggering instants, i.e., the fixed T in (11) becomes time-varying $T_k^i = t_{k+1}^i - t_k^i$. This requires that the event-triggering mechanism is Zeno-free, i.e., the inter-sample times T_k^i is positive, which is proved in Theorem 3. Furthermore, at the triggering instant t_k^i, only the local states, x_i, are updated and the last received states of the j^{th} subsystem should be used. This requires the Bellman error to be redefined as the event-driven Bellman error, $E_{ib,e}$.

The NN weight update law with the event-driven Bellman equation (23) is given by

$$\begin{aligned} \hat{\theta}_i^+(t) &= \hat{\theta}_i(t) - \alpha_{i1}(\partial E_{ib,e}/\partial\hat{\theta}_i)E_{ib,e}, \quad t = t_k^i \\ \dot{\hat{\theta}}_i(t) &= -\alpha_{i1}(\partial E_{ib,e}/\partial\hat{\theta}_i)E_{ib,e}, \quad t_k^i < t < t_{k+1}^i \end{aligned} \tag{24}$$

for $i = 1, 2, \ldots, N$, $\forall k$, where $\alpha_{i1} = \alpha_i/\rho_{ie}^2$ with the normalization term $\rho_{ie} = 1 + (\partial E_{ib,e}/\partial\hat{\theta}_i)^T(\partial E_{ib,e}/\partial\hat{\theta}_i)$ and $\hat{\theta}_i^+(t) = \hat{\theta}_i(t^+)$ evaluated at time $t = t_k^i, k \in \mathbb{N}$ and defined as $\lim_{s\to t}\hat{\theta}_i(s)$.

Remark 5: The significance of the hybrid impulsive learning approach in (24) is to accelerate the NN learning process by taking the advantage of the asynchronously received latest neighboring subsystem state information during the inter-sample intervals at each subsystem.

The event-triggering condition for asynchronous sampling and broadcasting is discussed in the following.

B. Event-Triggering Condition and Stability

An event-sampling mechanism is required at each subsystem to determine the broadcast instants for the system states. Consider a positive-definite, locally Lipschitz continuous function $L_i(x_i) \in \Re$ as the Lyapunov function of the i^{th} subsystem (1). The event-triggering condition using the Lyapunov function can be selected as

$$\|\bar{e}_i(t)\| \leq [(2 - e^{\gamma(t-t_k^i)})\beta_i - 1]L_i(x_i(t_k^i)), \quad t \in \left[t_k^i, t_{k+1}^i\right) \tag{25}$$

where $\beta_i > 1$, $\|\bar{e}_i(t)\| = P_{iL}\|e_i(t)\|$, and $\gamma > 0$ with $P_{iL} > 0$ is the Lipschitz constants satisfying $|L_i(x_i(t_k^i)) - L_i(x_i(t))| \leq P_{iL}\|e_i(t)\|$.

Lemma 3: If the inequality in (25) holds, then

$$L_i(x_i(t)) \leq (2 - e^{\gamma(t-t_k^i)})\beta_i L_i\left(x_i\left(t_k^i\right)\right), \quad t \in \left[t_k^i, t_{k+1}^i\right). \tag{26}$$

Proof: Refer to the Appendix.

Remark 6: Note that the triggering condition (25) derived based on the Lyapunov analysis ensures system stability in the inter-sample period. Furthermore, the event-sampling condition in (25) is decentralized as it is a function of local subsystem information and leads to an asynchronous sampling and transmission scheme. The condition (26) will be used in the stability analysis in place of (25) due to Lemma 3.

Define the augmented state vector $\chi_i = [x_i^T \ x_{ie}^T, \ \tilde{\theta}_i^T]^T$. The event-triggered system can be formulated as a nonlinear impulsive hybrid dynamical system [33] with flow dynamics corresponding to the inter-sample periods $t_k^i < t < t_{k+1}^i$, $\forall k, i$ and the jump dynamics at triggering instants $t = t_k^i$, $\forall k, i$. Using (1), (17), and (24), the impulsive dynamics can be obtained for $t_k^i < t < t_{k+1}^i$, $\forall k, i$ as

$$\dot{\chi}_i(t) = \begin{bmatrix} \bar{f}_i(x_i) + \bar{g}_i(x_i)\hat{u}_{ie} + \sum_{\substack{j=1 \\ j\neq i}}^{N} \Delta_{ij}(x_i, x_j) \\ 0 \\ \alpha_{i1}(\partial E_{ib,e}/\partial\hat{\theta}_i)E_{ib,e} \end{bmatrix} \tag{27}$$

$$\chi_i^{+}(t) = \begin{bmatrix} x_i(t) \\ x_i(t) \\ \tilde{\theta}_i + \alpha_{i1}(\partial E_{ib,e}/\partial\hat{\theta}_i)E_{ib,e} \end{bmatrix} \tag{28}$$

for $t = t_k^i$, $\forall k, i$.

Theorem 2: Consider the nonlinear event-based impulsive dynamics (27) and (28). Let Assumptions 1–5 hold, the initial control policy $u_i(0)$ be admissible, the critic NN weights initialized in a compact set, and updated according to (24). Suppose the initial event occurs at $t_0^i = 0$ and the system states are transmitted at the violation of the event-sampling condition (25). Then, the event-sampled control policy (22) renders the closed-loop impulsive dynamical system locally UB, provided the activation function and its gradient satisfy the PE condition with the design parameter $0 < \alpha_i < 1$.

Proof: Refer to the Appendix.

Corollary 2: Let the hypothesis of Theorem 2 holds. Then, the estimated value function (21) and control policy (22), respectively, converge to an arbitrarily close neighborhood of the optimal value function (19) and control policy (20), respectively.

Proof: Refer to the Appendix.

Next, the Zeno-free behavior of the event-sampling scheme is demonstrated.

Theorem 3: Let the hypothesis of Theorem 2 holds. Then, the inter-sample times $T_k^i = t_{k+1}^i - t_k^i$, $i = 1, 2, \ldots, N$, $\forall k$, for the sampling condition (25), are lower bounded such that

$$T_k^i > \frac{1}{\delta}\ln\left(\frac{\left(1 + \frac{\kappa_3}{\kappa_4}(2\beta_i - 1)L_i\left(x_i\left(t_k^i\right)\right)\right)}{\left(1 + \frac{\kappa_3}{\kappa_4}\beta_i L_i\left(x_i\left(t_k^i\right)\right)\right)}\right) > 0 \tag{29}$$

provided $\beta_i > 1$, where $\delta = \max\{\kappa_3, \gamma\}$ and $\kappa_3, \kappa_4 > 0$ are constants defined in the proof.

Proof: Refer to the Appendix.

C. Distributed Control of Linear Interconnected Systems

In this section, we discuss the implementation of the NZS-based control scheme presented in this paper for linear interconnected systems. The dynamics of the i^{th} subsystem in continuous time with linear dynamics are given by $\dot{x}_i(t) = \bar{A}_i x_i + \bar{B}_i u_i + \sum_{\substack{j=1 \\ j\neq i}}^{N} A_{ij}x_j$ for $i = 1, 2, \ldots, N$, where the linear map $A_i : \Re^{n_i} \to \Re^{n_i}$ and $\bar{B}_i : \Re^{n_i} \to \Re^{n_i \times m_i}$ are the internal dynamics and input gain of the i^{th} subsystem, respectively. The matrix function $A_{ij} : \Re^{n_i} \to \Re^{n_i \times n_j}$ represents the interconnection between the i^{th} and j^{th} subsystems.

The interconnected system can be represented as an N-player large-scale system given by $\dot{x}(t) = Ax + \sum_{j=1}^{N} B_j u_j, \quad x(0) = x_0$ where the map

$$A = \begin{bmatrix} \bar{A}_1 & \ldots & A_{1N} \\ \vdots & \ddots & \vdots \\ A_{N1}, & \ldots & A_{NN} \end{bmatrix}$$

and

$$B_j = [0, \ldots, \bar{B}_j^T, \ldots, 0]^T \in \Re^{n \times m_j}, \quad j = 1, \ldots, N$$

are the known overall internal dynamics and the control coefficient function, where 0s are the matrices of appropriate dimensions with all elements being zero.

The cost functional J_i associated with each subsystem for the admissible policies u_i, $i = 1, 2, \ldots, N$ is defined as $J_i(x) = \int_t^\infty (x^T Q_i x + \sum_{j=1}^{N} u_j^T R_{ij} u_j)d\tau$ where $Q_i > 0$ is a positive-definite matrix.

Let the candidate optimal value function be of the form $V_i^*(x) = (1/2)x^T(t)P_i^* x(t)$, $i = 1, 2, \ldots, N$, where $P_i^* > 0$ is a symmetric positive-definite matrix. The Hamiltonian function H_i is defined as

$$H_i\left(x, u_1, \ldots, u_N, V_{ix}^*\right) = x^T Q_i x + \sum_{j=1}^{N} u_j^T R_{ij} u_j + V_{ix}^{*T}\left[Ax(t) + \sum_{j=1}^{N} B_j u_j(t)\right] \tag{30}$$

where $V_{ix}^* = \partial V_i/\partial x = P_i^* x$. Applying the stationarity condition $\partial H_i/\partial u_i = 0$ reveals the greedy optimal u_i^* as

$$u_i^* = -\frac{1}{2} R_{ii}^{-1} B_i^T P_i^* x(t), \quad i = 1, 2, \ldots, N. \tag{31}$$

Inserting the optimal control policy (31) in the Hamiltonian function (30) reveals the coupled RE [34]. A forward-in-time solution to the coupled RE can be adaptively learned online using the ADP approach by representing the optimal value function as $V_i^*(x) = \theta_i^{*T} \bar{\phi}(x)$ where $\theta_i^* = \mathrm{vec}(P_i^*)$ is obtained using the vectorization of the matrix P_i^* and $\bar{\phi}(x) = \mathrm{vec}(x^T \otimes x)$ [35] where $\otimes$ is the Kronecker product.

Remark 7: Note that the regression vector is formed using the Kronecker product of the system state vector and, therefore, different from the bounded activation functions. Furthermore, the approximation error is not present.

In order to implement event-triggered control at each subsystem, similar to Section IV-B, the estimated control policy, parameter update law, and event-triggering conditions can be redefined, *mutatis-mutandis* and the stability of the linear interconnected system can be analyzed.

V. Simulation Results

In this section, three coupled nonlinear subsystems are considered for numerical verification of the algorithm. The three subsystems are the thigh and knee dynamics of a walking robot [25]. In the following, $x_1(t)$ is the relative angle between the two thighs, $x_2(t)$ is the right knee angle (relative to the right thigh), and $x_3(t)$ is the left knee angle (relative to left thigh). The controlled equations of motion (in units of rad/s) are: $\ddot{x}_1(t) = 0.1[1 - 5.25x_1^2(t)]\dot{x}_1(t) - x_1(t) + u_1(t)$

$$\begin{aligned}\ddot{x}_2(t) &= 0.01[1 - p_2(x_2(t) - x_{2\text{eq}})^2]\dot{x}_2(t) - 4(x_2(t) - x_{2\text{eq}}) \\ &\quad + 0.057x_1(t)\dot{x}_1(t) + 0.1(\dot{x}_2(t) - \dot{x}_3(t)) + u_2(t) \\ \ddot{x}_3(t) &= 0.01[1 - p_3(x_3(t) - x_{3\text{eq}})^2]\dot{x}_3(t) - 4(x_3(t) - x_{3\text{eq}}) \\ &\quad + 0.057x_1(t)\dot{x}_1(t) + 0.1(\dot{x}_3(t) - \dot{x}_2(t)) + u_3(t)\end{aligned}$$

where $\ddot{x}_i$ correspond to the dynamics of the i^{th} subsystem. The control objective is to bring the robot to a stop in a stable manner ($x_i \rightarrow x_{i\text{eq}}$), where $x_{i\text{eq}}$ are the equilibrium points with $x_{1\text{eq}} = 0, x_{2\text{eq}} = -0.227, x_{3\text{eq}} = 0.559$.

The parameters p_2 and p_3 are 6070 and 192, respectively. The NN to approximate V_i^* was designed with six hidden layer neurons. The initial conditions $x_i(0)$ and $\hat{\theta}_i(0)$ were selected randomly in the intervals $[-1, 1]$ and $[0, 1]$, respectively. The learning gains were selected for continuous-time simulations as $\alpha_1 = 25$, $\alpha_2 = 35$, and $\alpha_3 = 35$, and for the event-triggering case, $\alpha_1 = 0.4$, $\alpha_2 = 0.85$, and $\alpha_3 = 0.85$, $\beta_i = 1.086, \forall i \in \{1, 2, 3\}$. A quadratic performance index with $Q_i(x) = x^T \bar{Q}_i x$ is selected where the parameters $\bar{Q}_1 = 0.02$, $\bar{Q}_2 = 0.075$, $\bar{Q}_3 = 0.075$, $R_{11} = 0.04$, $R_{22} = 0.01$, $R_{33} = 0.01$, and $R_{ij} = R_{jj}$, for $i \neq j$, $i, j \in \{1, 2, 3\}$. The robotic system is simulated with the torques generated using the control algorithm with a hybrid leaning scheme. An exploratory random noise is included in the control policy to satisfy the PE condition during the initial learning phase for 2 s.

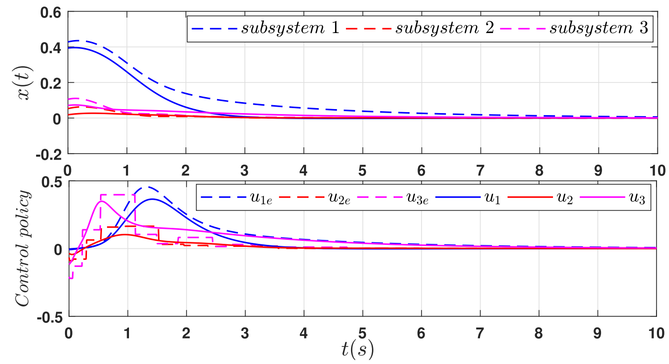

Fig. 1. Convergence of system states and control inputs for continuous (solid lines) and event-sampled system (dotted lines).

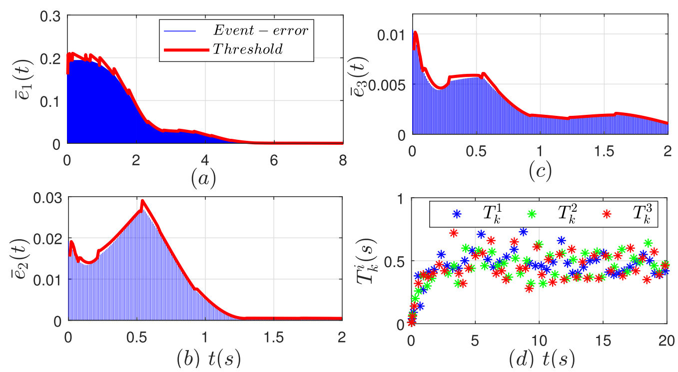

Fig. 2. Convergence of event-sampled error and threshold, and inter-sample times showing the asynchronous transmission instants.

The time history of the large-scale interconnected system states for both continuous (dotted) and event-based (solid) implementation is plotted in Fig. 1 (top). The system state vector both for the continuous and event-based designs converges to the equilibrium state with the approximated control policies. The control inputs for both the designs also converge to zero, as shown in Fig. 1 (bottom). The event-triggered control policies (dotted lines) are piecewise constant functions, since they are only updated at the triggering instants, and closely approximates the continuous policies.

To show the effectiveness of the event-based implementation in reducing communication and computation, the event-trigger error $\bar{e}_i(t)$ and the threshold in condition (25) for all the subsystems are shown in Fig. 2(a)–(c). Note that the event-triggering conditions are local and decentralized, and therefore, the thresholds are different for each subsystem leading to different number of sampling instants. In terms of number of events, highest number of triggering observed at the subsystem 1 and lowest at subsystem 2, implying asynchronous triggering at subsystems. The inter-sample times T_k^i are shown in Fig. 2(d). It is clear that the inter-sample times are different between two consecutive sampling instants leading to aperiodic sampling. This further implies that the computational and the communication resources are saved by reducing the transmission and controller execution when compared with periodic execution schemes.

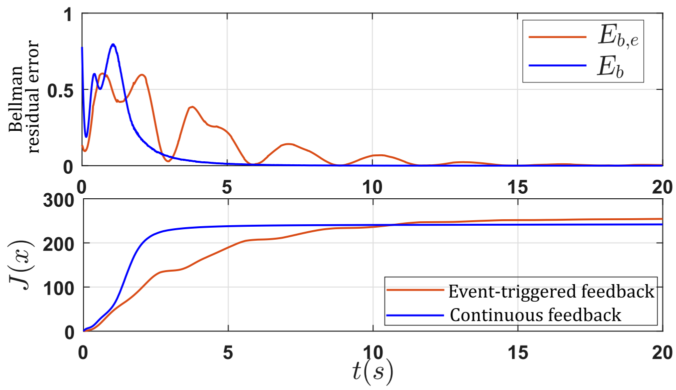

Fig. 3. Convergence of Bellman error and cumulative cost for continuous and event-sampled designs.

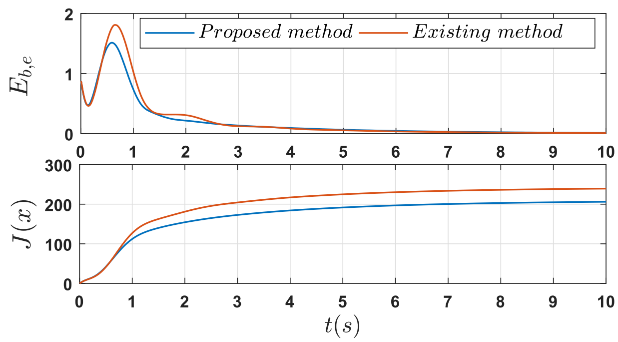

Fig. 4. Comparison of Bellman error and cumulative cost for the proposed method and the existing method [7].

From the near-optimality perspective, the Bellman residual errors for both continuous and event-based are shown in Fig. 3 (top), indicating the convergence of the errors to near-zero at the same time. This implies the estimated value function converged to its near-optimal value, and the Nash equilibrium solution is reached for both the cases. As expected, the time history of the event-based Bellman residual error is oscillating before convergence. This is due to the NN parameter update using the aperiodic feedback information with event-based sampling and transmission. The comparison between the cumulative cost, i.e., the total cost incurred for the convergence of the states, for a continuous and event-triggered solution is shown in Fig. 3 (bottom). It is clear that the event-based cost is slightly higher than the continuous implementation that demonstrates the tradeoff between the system performance and communication resource savings.

Finally, to compare the effectiveness of the proposed algorithm with the authors' previous work [7], the convergence of Bellman error and cumulative costs for the interconnected system are plotted in Fig. 4. The parameters in this experiment were chosen as follows: $\alpha_1 = 0.4$, $\alpha_2 = 0.85$, and $\alpha_3 = 0.85$, $\beta_i = 1.086, \forall i \in \{1, 2, 3\}$. A quadratic performance index with $Q_i(x) = x^T \bar{Q}_i x$ is selected where the parameters $\bar{Q}_1 = 0.05$, $\bar{Q}_2 = 0.085$, $\bar{Q}_3 = 0.085$, $R_{11} = 0.06$, $R_{22} = 0.07$, $R_{33} = 0.04$, and $R_{12} = -0.01$, $R_{13} = -0.002$, $R_{21} = -0.025$, $R_{23} = -0.003$, $R_{31} = -0.025$, $R_{32} = -0.01$. Note that the flexibility of the proposed distributed control framework lies in the additional term $\sum_{j=1,\, j\neq i}^{3} u_{ij}^T R_{ij} u_{ij}$, that is included in the cost function (2) of the i^{th} subsystem, as compared with the existing result [7], wherein $R_{ij} = 0$, $\forall i, j \in \{1, 2, 3\}$. In other words, due to the NZS framework, a tradeoff between the performance of different subsystems can be achieved by explicitly accounting for control policies of other neighboring subsystems while computing the control policy. From Fig. 4, the Bellman residual error for both the designs converges to near zero at the same time. Furthermore, it is clear that the proposed method incurs in lower cumulative cost than the existing method in [7]. This validates the effectiveness and difference of the proposed scheme.

VI. Conclusion

In this paper, a novel distributed optimal controller design for large-scale interconnected systems using an N-player NZS game is presented using the ADP-based scheme for both continuous and event-sampled implementation of control. Local UB of the system state vector and NN weight estimation errors are demonstrated analytically. It is observed from the simulation results that the hybrid learning scheme closely approximates the continuous time solution while saving the communication bandwidth. The proposed distributed optimal control scheme, formulated using the NZS game, offers flexibility in the achievable tradeoff between the performance of various subsystems. The optimization of the sampling intervals and communication constraints, such as delays and packet losses, are not considered during this design and will be included in our future work.

Appendix

Proof of Lemma 1: Consider the smooth, positive-definite function $L_i(\tilde{\theta}_i) = (1/2)\tilde{\theta}_i^T \tilde{\theta}_i$. The first derivative, $\dot{L}_i(\tilde{\theta}_i) = \tilde{\theta}_i^T \dot{\tilde{\theta}}_i$, along the dynamics of the NN weight estimation error (14), can be expressed as $\dot{L}_i(\tilde{\theta}_i) = \alpha_{i1}\tilde{\theta}_i^T(\partial E_{ib}/\partial\hat{\theta}_i)E_{ib}$. Using the Bellman equation (12) along with (9) reveals $E_{ib} = \hat{\theta}_i^T \Delta\phi(x, T) + \int_{t-T}^{t}(Q_i(x) + \sum_{j=1}^{N} u_j^T R_{ij} u_j)d\tau$ where $\Delta\phi(x, T) = (\phi(x(t)) - \phi(x(t-T)))$. Similarly, using (7) and (11), we have $\varepsilon_{ib} = \theta_i^{*T}\Delta\phi(x, T) + \int_{t-T}^{t}(Q_i(x) + \sum_{j=1}^{N} u_j^T R_{ij} u_j)d\tau$, where $\varepsilon_{ib} = \varepsilon_i(x(t)) - \varepsilon_i(x(t-T))$. From the above two relations and using the definition of $\tilde{\theta}_i$, one has

$$E_{ib} = -\tilde{\theta}_i^T \Delta\phi(x, T) + \varepsilon_{ib}. \tag{32}$$

Therefore, the Lyapunov time-derivative can be simplified as

$$\dot{L}_i(\tilde{\theta}_i) = -\alpha_{i1}\tilde{\theta}_i^T \Delta\phi(x, T)(\Delta\phi^T(x, T)\tilde{\theta}_i + \varepsilon_{ib}). \tag{33}$$

Applying Young's inequality for the term $\alpha_{i1}|\tilde{\theta}_i^T \Delta \phi(x, T)||\varepsilon_{ib}|$ to obtain $(\alpha_{i1}/2)\tilde{\theta}_i^T \Delta\phi(x, T)\Delta\phi^T(x, T)\tilde{\theta}_i + (\alpha_{i1}/2)\varepsilon_{ib}^T\varepsilon_{ib}$ reveals (15).

Proof of Theorem 1: Consider a continuously differentiable positive-definite candidate Lyapunov function $L : \Re^{l_\theta} \times B_x \to \Re$ given as $L(\tilde{\theta}, x) = \sum_{i=1}^{N} L_i(\tilde{\theta}_i, x_i)$, where $L_i(\tilde{\theta}_i, x_i) = \beta_i L_i(x_i) + L_i(\tilde{\theta}_i)$ is the Lyapunov function of the i^{th} subsystem with $\beta_i > 0$ and $L_i(\tilde{\theta}_i) = (1/2)\tilde{\theta}_i^T \tilde{\theta}_i$.

Considering the first term of the Lyapunov function, the first derivative $\dot{L}_i(x_i) = L_{ix_i}^T(x_i)\dot{x}_i$, along the system dynamics is

$$\dot{L}_i(x_i) = L_{ix_i}^T(x_i)\left[\bar{\bar{f}}_i(x) - \frac{1}{2}\bar{D}_i\nabla_x^T\phi(x)\hat{\theta}_i\right] \tag{34}$$

where $\bar{D}_i = g_i R_{ii}^{-1} g_i^T$. Note that, by Assumption 1, $\|\bar{D}_i\| \le \bar{D}_{iM}$. Expansion of the first derivative in (34) leads to

$$\dot{L}_i(x_i) = L_{ix_i}^T(x_i)\left[\left(\bar{\bar{f}}_i(x) + g_i u_i^*\right) + \frac{1}{2}\bar{D}_i\nabla_x\varepsilon_i\right] + \frac{1}{2}L_{ix_i}^T(x_i)\bar{D}_i\nabla_x^T\phi(x)\tilde{\theta}_i. \tag{35}$$

Combining (33) and (35) reveals

$$\begin{aligned}\dot{L}_i(\tilde{\theta}_i, x_i) = {}& \beta_i L_{ix_i}^T(x_i)\left[\left(\bar{\bar{f}}_i(x) + g_i u_i^*\right) + \frac{1}{2}\bar{D}_i\nabla_x\varepsilon_i\right] \\ &- \alpha_{i1}\tilde{\theta}_i^T\Delta\phi(x,T)\Delta\phi^T(x,T)\tilde{\theta}_i \\ &+ \alpha_{i1}\tilde{\theta}_i^T\Delta\phi(x,T)\varepsilon_{ib} + \frac{1}{2}\beta_i L_{ix_i}^T(x_i)\bar{D}_i\nabla_x^T\phi(x)\tilde{\theta}_i.\end{aligned} \tag{36}$$

Taking the summation on both the sides of (36), using (16), Young's inequality, and due to the PE conditions that there exists a $\bar{\tau}_{\min}$ such that $\inf_{\forall t}\{\lambda_{\min}(\Delta\phi(\cdot)\Delta\phi^T(\cdot)/((1+\Delta\phi^T(\cdot)\Delta\phi(\cdot))^2))\} = \bar{\tau}_{\min}$, where $\lambda_{\min}$ is the minimum Eigenvalue, we have

$$\begin{aligned}&\dot{L}(\tilde{\theta}, x) \\ &\le \sum_{i=1}^{N}\left\{-\left(\beta_i C_{i2} - (1+\bar{\tau}_{\min})\frac{\bar{D}_{iM}^2}{4}\right)\|L_{ix_i}(x_i)\|^2 \right. \\ &\qquad \left. -\left(\frac{\alpha_i}{2} - \frac{\nabla\phi_M^2\beta_i^2}{4}\right)\bar{\tau}_{\min}\tilde{\theta}_i^T\tilde{\theta}_i + \frac{\alpha_i}{2}\varepsilon_{ib}^T\varepsilon_{ib} + \beta_i^2\nabla\varepsilon_{iM}^2\right\}.\end{aligned} \tag{37}$$

From (37), for $\beta_i > (\bar{D}_{iM}^2/2C_{i2})$ and $\alpha_i > (\nabla\phi_M^2\beta_i^2/2)$, $\forall i$, the Lyapunov first derivative $\dot{L}(x,\tilde{\theta}) < 0$ as long as $\|L_{ix_i}(x_i)\|^2 > \bar{B}_{i\varepsilon}/(\beta_i C_{i2} - \bar{D}_{iM}^2/2) \equiv B_{x_i}$ or $2\bar{\tau}_{\min}\|\tilde{\theta}_i\|^2 > \bar{B}_{i\varepsilon}/(\alpha_i - \nabla\phi_M^2\beta_i^2/2) \equiv B_{\tilde{\theta}_i}$, where $\bar{B}_{i\varepsilon} = (\alpha_i/2)\varepsilon_{ib}^T\varepsilon_{ib} + \beta_i^2\nabla\varepsilon_{iM}^2$. Therefore, the system states and the NN weight estimation errors are UUB.

Proof of Corollary 1: Consider the error between the estimated value function and the optimal value function $\|\tilde{V}_i\| \le \|\tilde{\theta}_i^T\phi(x)\| + \|\varepsilon_i(x)\| \le \phi_M\|\tilde{\theta}_i\| + \varepsilon_{iM} \le B_{\tilde{V}}$. Similarly, the error between the optimal control policy and the estimated control policy is given by $\|\tilde{u}_i\| = \|\hat{u}_i - u_i^*\| \le (1/2)\lambda_{\max}(R_{ii}^{-1})g_{iM}(\nabla\phi_M\|\tilde{\theta}_i\| + \nabla\varepsilon_{iM}) \le B_{\tilde{u}}$, where $B_{\tilde{u}} > 0$. From the proof of Theorem 1, the NN weight estimation error $\tilde{\theta}_i$ is bounded and with Assumption 4, $\|\tilde{V}_i\|$ and $\|\tilde{u}_i\|$ are UUB. Since the bound can be made smaller by increasing the number of neurons, the estimated value and the estimated Nash solution, consequently, converge to the neighborhood of their optimal values, respectively.

Proof of Lemma 3: By Lipschitz continuity of the Lyapunov function $L_i(x_i(t))$, it holds that $|L_i(x_i(t)) - L_i(x_i(t_k^i))| \le P_{iL}\|x_i(t) - x_i(t_k^i)\| = P_{iL}\|e_i(t)\|$, $t \in [t_k^i, t_{k+1}^i)$.

As per the Lemma statement, since the inequality (25) holds, the above inequality satisfies $|L_i(x_i(t)) - L_i(x_i(t_k^i))| \le (2 - e^{\gamma(t-t_k^i)})\beta_i L_i(x_i(t_k^i)) - L_i(x_i(t_k^i))$. Adding $L_i(x_i(t_k^i))$ top both the sides and using triangle inequality lead to (26).

Proof of Theorem 2 (Flow Dynamics): Consider a continuously differentiable positive-definite candidate Lyapunov function, $L(\chi)$, and given as $L(\chi) = \sum_{i=1}^N L_i(\chi_i)$, where $L_i(\chi_i) = \chi_i^T\hat{\beta}_i\chi_i$ with $\hat{\beta}_i = \operatorname{diag}(\beta_i, \beta_i, 1)$. Therefore, $L_i(\chi_i) = L_i(\tilde{\theta}_i) + \beta_i L_i(x_i) + \beta_i L_i(x_{i,e})$ is the Lyapunov function of the i^{th} subsystem where $L_i(\tilde{\theta}_i) = (1/2)\tilde{\theta}_i^T\tilde{\theta}_i$, $L_i(x_i) = x_i^T x_i$, $L_i(x_{i,e}) = x_{i,e}^T x_{i,e}$, and $\beta_i > 1$. Taking the time-derivative and using the dynamics (27), we have $\dot{L}_i(x_{i,e}) = 0$, and from Lemma 3, $L_i(x_i) \le (2 - e^{\gamma(t-t_k^i)})\beta_i L_i(x_i(t_k^i))$. With $t_0^i = 0, \forall i$, the first derivative

$$\dot{L}_i(x_i) \le -e^{\gamma(t-t_k^i)}\beta_i L_i\left(x_i\left(t_k^i\right)\right). \tag{38}$$

Finally, $\dot{L}_i(\tilde{\theta}_i) = \tilde{\theta}_i^T\dot{\tilde{\theta}}_i$. Using the weight tuning rule, $\dot{L}_i(\tilde{\theta}_i) = \alpha_{i1}\tilde{\theta}_i^T(\partial E_{ib,e}/\partial\hat{\theta}_i)E_{ib,e}$. Substituting (19) in (11) and (21) in (23), we get the Bellman equations in parametric form, with the optimal value function and the estimated value function, in the event-triggered feedback framework. Then, similar to (32), in the event-triggered feedback framework, we have $E_{ib,e} = -\tilde{\theta}_i^T\Delta\phi(x_e, T) + \varepsilon_{ib,e}$.

Substituting $E_{ib,e}$ in $\dot{L}_i(\tilde{\theta}_i)$, we have

$$\dot{L}_i(\tilde{\theta}_i) = -\alpha_{i1}\tilde{\theta}_i^T\Delta\phi(x_e, T)(\Delta\phi^T(x_e, T)\tilde{\theta}_i + \varepsilon_{ib,e}). \tag{39}$$

Similar to the steps in Lemma 1, we get

$$\dot{L}_i(\tilde{\theta}_i) \le -\frac{\alpha_{i1}}{2}\left(\tilde{\theta}_i^T\Delta\phi(x_e)\Delta\phi^T(x_e)\tilde{\theta}_i + \varepsilon_{ib,e}^T\varepsilon_{ib,e}\right). \tag{40}$$

Combining the Lyapunov time-derivative for the weight estimation error (40) and the states (38) reveals

$$\dot{L}_i(\chi_i) \le -e^{\gamma(t-t_k^i)}\beta_i L_i(x_i(t_k^i)) - \frac{\alpha_{i1}}{2}\tilde{\theta}_i^T\Delta\phi(x_e)\Delta\phi^T(x_e)\tilde{\theta}_i + \frac{\alpha_i}{2}\varepsilon_{ib,e}^T\varepsilon_{ib,e}. \tag{41}$$

Therefore, it can be concluded that for $\alpha_i > 0$, $\dot{L}_i(\chi_i)$ is bounded for $i = 1, \ldots, N$ in the flow-period and the bounds are the functions of approximation errors.

Jump Dynamics: Consider the Lyapunov function from the flow period. Along the jump dynamics (28), the system state $x_i^+ = x_i$. Therefore, the first difference $\Delta L_i(x_i) = L_i(x_i^+) - L_i(x_i) = 0$. Again from the jump dynamics (28), the sampled state $x_{i,e}^+ = x_i(t_k^i) = x_{i,e}(t_{k+1}^i)$. Therefore, the first difference for the second term in the Lyapunov function $\Delta L_i(x_{i,e}) = L_i(x_{i,e}^+) - L_i(x_{i,e}) = L_i(x_{i,e}(t_{k+1}^i)) - L_i(x_{i,e}(t_k^i))$. From the fact that the initial sampling is at $t_0^i = 0$ and the system state converges to the a bound defined by $(\alpha_i/2)\varepsilon_{ib,e}^T\varepsilon_{ib,e} = B_i$ during the inter-sample times, as proved in the flow-dynamics, so, it holds that $x_i(t_{k+1}^i) \le x_i(t_k^i)$, when $\|L_i(x_i)\| > e^{-\gamma(t-t_k^i)}B_i/\beta_i$. Hence, there exist a constant $C_1 > 0$ such that $\Delta L_i(x_{i,e}) = L_i(x_{i,e}(t_{k+1}^i)) - L_i(x_{i,e}(t_k^i)) \le -C_1\|x_{i,e}(t_{k+1}^i) - x_{i,e}(t_k^i)\|$.

Finally, $\Delta L_i(\tilde{\theta}_i) = (1/2)\tilde{\theta}_i^{+T}\tilde{\theta}_i^+ - (1/2)\tilde{\theta}_i^T\tilde{\theta}_i$. Using the error jump-dynamics, we have $\Delta L_i(\tilde{\theta}_i) = 2\alpha_{i1}\tilde{\theta}^T(\partial E_{ib,e}/$

$\partial\hat{\theta}_i)E_{ib,e} + \alpha_{i1}(\partial E_{ib,e}{}^T/\partial\hat{\theta}_i)E_{ib,e}\alpha_{i1}(\partial E_{ib,e}/\partial\hat{\theta}_i)E_{ib,e}$. Following the analysis similar to the flow dynamics:

$$\Delta L_i(\tilde{\theta}_i) \le -\alpha_{i1}\tilde{\theta}_i^T\Delta\phi(x_e,T)\Delta\phi^T(x_e,T)\tilde{\theta}_i + \alpha_i\varepsilon_{ib,e}^T\varepsilon_{ib,e} + \alpha_{i1}^2\tilde{\theta}_i^T(\Delta\phi(x_e,T)\Delta\phi^T(x_e,T))^2\tilde{\theta}_i.$$

Since $a^2/(1+a^2) \le 1,\ \forall a > 0$, and recalling the PE condition as in Theorem 1, we can conclude that $\Delta L_i(\tilde{\theta}_i) \le -\alpha_{i1}(1-\alpha_i)\bar{\tau}_{\min}\|\tilde{\theta}_i\|^2 + \alpha_i\varepsilon_{ib,e}^T\varepsilon_{ib,e}$.

Therefore, for $0 < \alpha_i < 1$, the closed-loop system is bounded during the jump instants. Combining the results from the flow and jump dynamics, it can be concluded that the closed-loop states of each subsystem and the weight estimation errors at each subsystem remain bounded for all times. The overall states and weight estimation error bounds can be obtained similar to Theorem 1.

Proof of Theorem 3: The dynamics of the event-trigger error satisfies $(d\|\bar{e}_i\|/dt) \le \|\dot{\bar{e}}_i\| = \|P_{iL}\dot{x}_i\| \le P_{if\Delta}(\|\bar{e}_i\| + \|\bar{e}_j\|) + \kappa_1\|\bar{e}_i\| + \kappa_2$, where $\|\bar{\bar{f}}_i(x) - \bar{\bar{f}}_i(x_e)\| \le P_{if\Delta}\|e(t)\|$ with $P_{if\Delta} > 0$, $\kappa_1 = (1/2)L_{ig}\lambda_{\max}(R_{ii}^{-1})\bar{g}_{iM}\nabla_x^T\phi_M\hat{\theta}_{iM}$, and $\kappa_2 = \|\bar{\bar{f}}(x_{ie})\| + (1/2)P_{iL}\bar{D}_{ieM}\nabla_x^T\phi_M\hat{\theta}_{iM}$ with $\bar{D}_{ie} = \bar{g}_i(x_{ie})R_{ii}^{-1}\bar{g}_i(x_{ie})$, $\|\bar{D}_{ie}\| \le \bar{D}_{ieM}$, and $\|\bar{g}_i(x_i) - \bar{g}_i(x_{ie})\| \le L_{ig}\|e_i\|$. The above inequality is reached using the Lipschitz continuity of the function $\bar{\bar{f}}_i(x)$ and $\bar{g}_i(x)$.

Recalling the event-triggering condition (25) for the j^{th} subsystem, the above equation can be expressed as $\|\dot{\bar{e}}_i\| \le \kappa_3\|\bar{e}_i\| + \kappa_4$, where $\kappa_3 = P_{if\Delta} + \kappa_1$ and $\kappa_4 = \kappa_2 + P_{jf\Delta}\|(\beta_j - 1)L_j(x_j(t_k^j))\|$. Note that κ_4 is constant during the inter-sample times. By comparison lemma, the solution of $\|\dot{\bar{e}}_i(t)\|$ with $\|\bar{e}_i(t_k^i)\| = 0$ is upper bounded by

$$\|\bar{e}_i(t)\| \le \int_{t_k^i}^{t}\kappa_4 e^{\kappa_3(t-\tau)}d\tau = \frac{\kappa_4}{\kappa_3}\left(e^{\kappa_3}\left(t - t_k^i\right) - 1\right). \quad (42)$$

At the next sampling instant, $\|\bar{e}_i(t_{k+1}^i)\| = ((1 - e^{\gamma(t_{k+1}^i - t_k^i)})\beta_i - 1)L_i(x_i(t_k^i))$. Comparing both the equations, we have $\|\bar{e}_i(t_{k+1}^i)\| = ((2 - e^{\gamma(t_{k+1}^i - t_k^i)})\beta_i - 1)L_i(x_i(t_k^i)) \le (\kappa_4/\kappa_3)(e^{\kappa_3(t_{k+1}^i - t_k^i)} - 1)$.

Solving the equation for the inter-sample time with $\delta = \max\{\kappa_3, \gamma\}$ leads to (29).

References

[1] D. Wang, C. Mu, H. He, and D. Liu, "Event-driven adaptive robust control of nonlinear systems with uncertainties through NDP strategy," *IEEE Trans. Syst., Man, Cybern., Syst.*, vol. 47, no. 7, pp. 1358–1370, Jul. 2017.

[2] H. Xu and S. Jagannathan, "Neural network-based finite horizon stochastic optimal control design for nonlinear networked control systems," *IEEE Trans. Neural Netw. Learn. Syst.*, vol. 26, no. 3, pp. 472–485, Mar. 2015.

[3] S. Mehraeen and S. Jagannathan, "Decentralized optimal control of a class of interconnected nonlinear discrete-time systems by using online Hamilton-Jacobi-Bellman formulation," *IEEE Trans. Neural Netw.*, vol. 22, no. 11, pp. 1757–1769, Nov. 2011.

[4] D. Liu, D. Wang, and H. Li, "Decentralized stabilization for a class of continuous-time nonlinear interconnected systems using online learning optimal control approach," *IEEE Trans. Neural Netw. Learn. Syst.*, vol. 25, no. 2, pp. 418–428, Feb. 2014.

[5] Y. Liu and X.-Y. Li, "Decentralized robust adaptive control of nonlinear systems with unmodeled dynamics," *IEEE Trans. Autom. Control*, vol. 47, no. 5, pp. 848–856, May 2002.

[6] S. Huang, K. K. Tan, and T. H. Lee, "Decentralized control design for large-scale systems with strong interconnections using neural networks," *IEEE Trans. Autom. Control*, vol. 48, no. 5, pp. 805–810, May 2003.

[7] V. Narayanan and S. Jagannathan, "Event-triggered distributed approximate optimal state and output control of affine nonlinear interconnected systems," *IEEE Trans. Neural Netw. Learn. Syst.*, vol. 29, no. 7, pp. 2846–2856, Jul. 2018.

[8] K. S. Narendra and S. Mukhopadhyay, "To communicate or not to communicate: A decision-theoretic approach to decentralized adaptive control," in *Proc. Amer. Control Conf. (ACC)*, 2010, pp. 6369–6376.

[9] H. Ma, Z. Wang, D. Wang, D. Liu, P. Yan, and Q. Wei, "Neural-network-based distributed adaptive robust control for a class of nonlinear multiagent systems with time delays and external noises," *IEEE Trans. Syst., Man, Cybern., Syst.*, vol. 46, no. 6, pp. 750–758, Jun. 2016.

[10] X. Wang and M. D. Lemmon, "Event-triggering in distributed networked control systems," *IEEE Trans. Autom. Control*, vol. 56, no. 3, pp. 586–601, Mar. 2011.

[11] R. Singh, P. R. Kumar, and L. Xie, "Decentralized control via dynamic stochastic prices: The independent system operator problem," *IEEE Trans. Autom. Control*, to be published, doi: 10.1109/TAC.2018.2799899.

[12] D. D. Šiljak, *Decentralized Control of Complex Systems*. Chelmsford, MA, USA: Courier Corporation, 2011.

[13] O. Tutsoy and S. Colak, "Adaptive estimator design for unstable output error systems: A test problem and traditional system identification based analysis," *Proc. Inst. Mech. Eng. I, J. Syst. Control Eng.*, vol. 229, no. 10, pp. 902–916, Nov. 2015.

[14] R. Bellman, *Dynamic Programming*. Chelmsford, MA, USA: Courier Corporation, 2013.

[15] T. Dierks and S. Jagannathan, "A self-tuning optimal controller for affine nonlinear continuous-time systems with unknown internal dynamics," in *Proc. 51st IEEE Conf. Decis. Control (CDC)*, Dec. 2012, pp. 5392–5397.

[16] A. Heydari, "Stability analysis of optimal adaptive control under value iteration using a stabilizing initial policy," *IEEE Trans. Neural Netw. Learn. Syst.*, vol. 29, no. 9, pp. 4522–4527, Sep. 2018.

[17] K. Rajagopal, S. N. Balakrishnan, and J. R. Busemeyer, "Neural network-based solutions for stochastic optimal control using path integrals," *IEEE Trans. Neural Netw. Learn. Syst.*, vol. 28, no. 3, pp. 534–545, Mar. 2017.

[18] R. S. Sutton and A. G. Barto, *Reinforcement Learning—An Introduction*. Cambridge, MA, USA: MIT Press, 1998.

[19] B. Kiumarsi, K. G. Vamvoudakis, H. Modares, and F. L. Lewis, "Optimal and autonomous control using reinforcement learning: A survey," *IEEE Trans. Neural Netw. Learn. Syst.*, vol. 29, no. 6, pp. 2042–2062, Jun. 2018.

[20] H. S. Witsenhausen, "A counterexample in stochastic optimum control," *SIAM J. Control*, vol. 6, no. 1, pp. 131–147, 1968.

[21] P. Tabuada, "Event-triggered real-time scheduling of stabilizing control tasks," *IEEE Trans. Autom. Control*, vol. 52, no. 9, pp. 1680–1685, Sep. 2007.

[22] A. Sahoo, V. Narayanan, and S. Jagannathan, "Optimal sampling and regulation of uncertain interconnected linear continuous time systems," in *Proc. IEEE Symp. Ser. Comput. Intell. (SSCI)*, Nov./Dec. 2017, pp. 1–6.

[23] L. Dong, X. Zhong, C. Sun, and H. He, "Event-triggered adaptive dynamic programming for continuous-time systems with control constraints," *IEEE Trans. Neural Netw. Learn. Syst.*, vol. 28, no. 8, pp. 1941–1952, Aug. 2017.

[24] T. Liu and Z. P. Jiang, "A small-gain approach to robust event-triggered control of nonlinear systems," *IEEE Trans. Autom. Control*, vol. 60, no. 8, pp. 2072–2085, Aug. 2015.

[25] V. Narayanan and S. Jagannathan, "Approximate optimal distributed control of uncertain nonlinear interconnected systems with event-sampled feedback," in *Proc. IEEE 55th Conf. Decis. Control (CDC)*, Dec. 2016, pp. 5827–5832.

[26] V. Narayanan and S. Jagannathan, "Distributed adaptive optimal regulation of uncertain large-scale linear networked control systems using Q-learning," in *Proc. IEEE Symp. Ser. Comput. Intell.*, Dec. 2015, pp. 587–592.

[27] A. W. Starr and Y. C. Ho, "Nonzero-sum differential games," *J. Optim. Theory Appl.*, vol. 3, no. 3, pp. 184–206, Mar. 1969.

[28] J. Nash, "Non-cooperative games," *Ann. Math.*, vol. 54, no. 2, pp. 286–295, 1951.

[29] K. G. Vamvoudakis and F. L. Lewis, "Multi-player non-zero-sum games: Online adaptive learning solution of coupled Hamilton–Jacobi equations," *Automatica*, vol. 47, no. 8, pp. 1556–1569, Aug. 2011.

[30] M. Johnson, R. Kamalapurkar, S. Bhasin, and W. E. Dixon, "Approximate n-player nonzero-sum game solution for an uncertain continuous nonlinear system," *IEEE Trans. Neural Netw. Learn. Syst.*, vol. 26, no. 8, pp. 1645–1658, Aug. 2015.
[31] F. Lewis, S. Jagannathan, and A. Yeşildirak, *Neural Network Control of Robot Manipulators and Nonlinear Systems*. Philadelphia, PA, USA: Taylor & Francis, 1999.
[32] A. Sahoo, H. Xu, and S. Jagannathan, "Neural network-based adaptive event-triggered control of nonlinear continuous-time systems," in *Proc. IEEE Int. Symp. Intell. Control (ISIC)*, Aug. 2013, pp. 35–40.
[33] W. M. Haddad, V. Chellaboina, and S. G. Nersesov, *Impulsive and Hybrid Dynamical Systems: Stability, Dissipativity, and Control*. Princeton, NJ, USA: Princeton Univ. Press, 2006.
[34] R. Song, F. L. Lewis, and Q. Wei, "Off-policy integral reinforcement learning method to solve nonlinear continuous-time multiplayer nonzero-sum games," *IEEE Trans. Neural Netw. Learn. Syst.*, vol. 28, no. 3, pp. 704–713, Mar. 2017.
[35] F. L. Lewis, D. Vrabie, and V. L. Syrmos, *Optimal Control*, 3rd ed. Hoboken, NJ, USA: Wiley, 2012.

Vignesh Narayanan (M'17) received the B.Tech. degree in electrical engineering from SASTRA University, Thanjavur, India, in 2012, and the master's degree in electrical engineering from the National Institute of Technology, Kurukshetra, India, in 2014, and the Ph.D. degree from Missouri University of Science and Technology, Rolla, MO, USA, in 2017.

He is currently a Post-Doctoral Fellow with Washington University in St. Louis, St. Louis, MO, USA. His current research interests include neural network control, learning, and adaptive systems.

Avimanyu Sahoo (M'15) received the master's degree in electrical engineering from IIT Varanasi, India, in 2011, and the Ph.D. degree in electrical engineering from the Missouri University of Science and Technology, Rolla, MO, USA, in 2015.

He is currently an Assistant Professor with Oklahoma State University, Stillwater, OK, USA. His current research interests include event-sampled control, adaptive control, neural network control, networked control system, and optimal control.

Sarangapani Jagannathan (F'16) was a Site Director for the NSF Industry/University Cooperative Research Center on Intelligent Maintenance Systems for 13 years. He is currently a Rutledge-Emerson Distinguished Professor of electrical and computer engineering with the Missouri University of Science and Technology (former University of Missouri-Rolla), Rolla, MO, USA. He has co-authored with his students 157 peer-reviewed journal articles, 271 refereed IEEE conference articles, several book chapters, authored/co-edited six books. He holds 20 U.S. patents, one patent defense publication, and several pending. He graduated 29 Ph.D. and 30 M.S. thesis students, and his total funding is in excess of $17 million with over $9.5 million toward his shared credit from federal and industrial entities. His current research interests include neural network control, adaptive event-triggered control/cyber-physical systems, prognostics, and autonomous systems/robotics.

Dr. Jagannathan was a recipient of many awards including the 2018 IEEE CSS Transition to Practice Award, the 2007 Boeing Pride Achievement Award, the 2000 NSF Career Award, and the 2001 Caterpillar Research Excellence Award. He was a Co-Editor for the IET book series on control from 2010 until 2013 and now serving on many editorial boards including IEEE Systems, Man and Cybernetics. He has been on organizing committees of several IEEE Conferences. He is a Fellow of Institute of Measurement and Control, U.K., and the Institution of Engineering and Technology, U.K.

Koshy George (SM'05) received the B.E. degree in electrical and electronics engineering from the University of Mysore, Mysuru, India, the M.S. degree in electrical engineering from IIT Madras, Chennai, India, and the Ph.D. degree in engineering from the Indian Institute of Science, Bengaluru, India.

He is currently a Professor of electronics and communications engineering with PES University, Bengaluru, where he is also the Director of the PES Centre for Intelligent Systems. His current research interests include adaptive systems and nonlinear systems.